In: Proceedings of the *5th IEEE Southwest Symposium on Image Analysis and Interpretation*, 206-210, 2002.

# Analysis of motion and curvature in image sequences *

Erhardt Barth
Institute for Neuro- and Bioinformatics, University of Lübeck
Ratzeburger Allee 160, 23538 Lübeck, Germany
barth@inb.mu-luebeck.de, www.inb.mu-luebeck.de

Ingo Stuke
Institute for Signal Processing, University of Lübeck
stuke@isip.mu-luebeck.de

Cicero Mota
University of Amazonas, Brazil
mota@impa.br

## Abstract

*We briefly review a recent development in the area of computer vision and multidimensional signal processing. Image sequences are regarded as hypersurfaces and useful properties are derived from the geometry of that hypersurface. Besides demonstrating the uniqueness of curvature, new methods for the analysis of single and multiple motions are presented including the case of occluded motions.*

## 1. Introduction

Light intensity $f$ as a function of space and time defines a hypersurface

$$S = (x, y, t, f(x, y, t)) \tag{1}$$

that has the form of a three-dimensional Monge patch. From a geometric point of view the curvature is the most important property of the surface in that it determines the intrinsic structure of the manifold [13]. Geometric methods in computer vision most often deal with the extrinsic geometry of objects in 3D space and how these objects and their motions project on the image plane. However, the geometry of the hypersurface $S$ has been used for motion detection [10] with an algorithm based on the gradient of $f$. It has also been shown how the Gaussian curvature of $S$ can be used to detect motion discontinuities [18].

We will consider the curvature tensor and the structure tensor of $S$ and relate them to motion parameters. Various methods for motion estimation are known and comprehensive reviews can be found, e.g., in [2, 9].

*Work supported in parts by the DAAD under A/99/22641 and the DFG under Ba 1176/7-1.

Less well understood is the problem of dealing with multiple motions that can occur in computer-vision applications, e.g., in case of semi-transparencies and occlusions, and also in medical imaging, when different layers of tissue move differently. An overview of the problem of multiple motions has been given in [7]. To our knowledge, the problem of two motions has been first solved in [14] by the use of spatio-temporal Gabor filters and fourth-order moments derived from these filters. The main differences to our approach are that we do not need to solve a six-dimensional eigensystems, that we can extend our approach to more than two motions, and that we obtain a higher resolution with less regularization. A recent analysis of the spectral properties of multiple motions can be found in [17]. Others have introduced the useful and intuitive notions of 'nulling filters' and 'layers' [15, 16]. Their approach is more general in that it treats the separation of motions into layers, but is also limited to the use of a discrete set of possible motions and a probabilistic procedure for finding the most likely motions out of the set.

## 2. Curvature of image sequences

In case of image sequences, curvature is measured by the Riemann curvature tensor that has six independent components in 3D. For a surface of type (1) the components are

$$\begin{aligned}
R_{2121} &= (f_{yy}f_{xx} - {f_{xy}}^2)/(1 + \vec{\nabla}{f}^2) \\
R_{3131} &= (f_{tt}f_{xx} - {f_{xt}}^2)/(1 + \vec{\nabla}f^2) \\
R_{3232} &= (f_{tt}f_{yy} - {f_{yt}}^2)/(1 + \vec{\nabla}f^2) \\
R_{3121} &= (f_{yt}f_{xx} - f_{xt}f_{xy})/(1 + \vec{\nabla}f^2) \\
R_{3221} &= (f_{yt}f_{xy} - f_{yy}f_{xt})/(1 + \vec{\nabla}f^2) \\
R_{3231} &= (f_{tt}f_{xy} - f_{xt}f_{yt})/(1 + \vec{\nabla}f^2) \\
\text{with:} 1 + \vec{\nabla}f^2 &= 1 + {f_x}^2 + {f_y}^2 + {f_t}^2
\end{aligned} \tag{2}$$

A surface is said to be curved at a point if the Riemann tensor does not vanish or, equivalently, if it has a non-zero component. The component $R_{1212}$ is the 2D Gaussian curvature of the section $t = t_0$, except for a slightly different denominator, i.e., $R_{1212}$ is the curvature of single images. Since it has been shown that curved image regions uniquely specify a surface [4, 11], flat image regions (that are not curved, e.g. straight edges) are redundant. The components $R_{1313}(y = y_0)$ and $R_{2323}(x = x_0)$ are also sectional curvatures in $(x, t)$ and $(y, t)$ respectively. Therefore, the whole surface is curved at any place where the section $t = t_0$ is, i.e., the region of non-zero curvature of the whole hypersurface contains the set of non-zero curvatures of the sections $t = t_0$. From this last fact, one can derive the redundancy of flat regions in three-dimensional hypersurface from the two dimensional case [11]. These results are important in the context of image compression and feature extraction for computer-vision systems.

The curvature as defined above is built on second-order derivatives. We now construct similar measures based on first-order derivatives of $f$. We first define the following matrix:

$$\mathbf{D}(x, y, t) = (\vec{\nabla} f)^T (\vec{\nabla} f) = \begin{pmatrix} {f_x}^2 & f_x f_y & f_x f_t \\ f_x f_y & {f_y}^2 & f_y f_t \\ f_x f_t & f_y f_t & {f_t}^2 \end{pmatrix}. \tag{3}$$

Since this matrix does not contain more information than the gradient $(f_x, f_y, f_t)$ itself, a different matrix, obtained from $\mathbf{D}$ by convolution with a smoothing kernel $h(x, y)$ (or $h(x, y, t)$), i.e.

$$\mathbf{J}(x, y, t) = h(x, y) * \mathbf{D}(x, y, t), \tag{4}$$

can be used to characterize the structure of $f(x, y, t)$. Accordingly, $\mathbf{J}$ has been called "structure tensor" - see [8, 9] for a review.

We now consider the minors of $\mathbf{J}$, i.e. the matrix

$$\mathbf{M} = \mathrm{Minors}(\mathbf{J}). \tag{5}$$

The elements $M_{ij}, (i, j = 1, 2, 3)$ of $\mathbf{M}$ are the determinants of the matrices obtained from $\mathbf{J}$ by eliminating the row $4 - i$ and the column $4 - j$, e.g., $M_{11} = (h * {f_x}^2)(h * {f_y}^2) - (h*(f_x f_y))^2$. $\mathbf{J}$ is a symmetric, positive semidefinite matrix and the following numbers are invariants of $\mathbf{J}$:

$$\begin{array}{ll} K & = \det \mathbf{J} = \lambda_1 \lambda_2 \lambda_3 \\ S & = (M_{11} + M_{22} + M_{33})/3 \\ & = (\lambda_1 \lambda_2 + \lambda_1 \lambda_3 + \lambda_2 \lambda_3)/3 \\ H & = (\mathrm{trace}\mathbf{J})/m = (\lambda_1 + \lambda_2 + \lambda_3)/3 \end{array} \tag{6}$$

with $\lambda_i$ being the eigenvalues of $\mathbf{J}$. The structure tensor $\mathbf{J}$ (4) is the metric of the immersion $F(x, y, t) = (f(x - x_1, y - y_1, t), \ldots, f(x - x_s, y - y_s, t))$, where $(x_s, y_s)$ are the sampling points for the image sequence $f$. The measures $K$, $S$ and $H$ are metric invariants of this immersion and are related to the Gaussian, scalar, and mean curvatures of the manifold $F$ respectively. Furthermore, the minors of $\mathbf{J}$ are related to the components of the Riemann curvature tensor. The precise nature of these relations is beyond the scope of this paper.

## 3. Curvature and motion

**Translation with constant velocity** If the image sequence $f(x, y, t)$ results from a spatial pattern moving with constant velocity $\mathbf{v} = (v_x, v_y)$, $f$ is assumed to satisfy the constraint [1]

$$f(x, y, t) = f(x + dx, y + dy, t + dt), \tag{7}$$

that leads to [1]

$$\alpha(\mathbf{v}) f = 0 \tag{8}$$

where $\alpha(\mathbf{v}) = v_x \frac{\partial}{\partial x} + v_y \frac{\partial}{\partial y} + \frac{\partial}{\partial t}$ is the derivative operator along $\mathbf{V} = (v_x, v_y, 1)$. The solution of (8) is

$$f(x, y, t) = f(x - v_x t, y - v_y t). \tag{9}$$

Between the components of the curvature tensor (2), evaluated for the specific function $f$ in Eq. (9), the following results hold [6]:

$$\begin{array}{ll} \mathbf{v} & = \mathbf{v}_1 = (R_{3221}, -R_{3121})/R_{2121} \\ \mathbf{v} & = \mathbf{v}_2 = (R_{3231}, -R_{3131})/R_{3121} \\ \mathbf{v} & = \mathbf{v}_3 = (R_{3232}, -R_{3231})/R_{3221}. \end{array} \tag{10}$$

Indices simply denote the fact that we obtain different expressions for $\mathbf{v}$.

In analogy, we obtain the following relations for the minors of $\mathbf{J}$ [3]:

$$\mathbf{v} = \mathbf{v}_i = (M_{3i}, -M_{2i})/M_{1i}, i = 1, 2, 3. \tag{11}$$

To better understand these results, we recall that motion estimation is often treated as an optimization problem, e.g. by using least-squares methods. The optimization problem then leads to an eigenvalue problem, for example in the case of the tensor-based methods where the motion vector is computed as the eigenvector to the zero eigenvalue - see [8, 9] for a review. Since it is known that if a matrix has a single zero eigenvalue, the corresponding eigenvector can be evaluated in terms of the minors of that matrix [12], we can easily relate the result in Eq. (11) to the methods that use the eigenvectors of $\mathbf{J}$. However, the method based on the minors has been shown to be faster and more accurate [3].

**Translation with time-dependent velocity** We now consider the more general case where the image shift contains higher-order terms, i.e., the motion can be accelerated, i.e.,

$$f(x, y, t) = f(x - d_x(t), y - d_y(t)). \quad (12)$$

With the constraint in Eq. 12, we still obtain for the curvature tensor (note that $(d'_x, d'_y) = \mathbf{v}$)

$$(R_{3221}, -R_{3121})/R_{2121} = (d'_x(t), d'_y(t)), \quad (13)$$

but the expressions $(R_{3231}, -R_{3131})/R_{3121}$, $(R_{3232}, -R_{3231})/R_{3221}$ do not simplify to yield the velocity components (due to non-vanishing second-order derivatives) - see [5] for a more comprehensive analysis.

The minors of **J** do not involve second-order derivatives, therefore under the constraint (12) we obtain the same results as in Eq. (11) with $\mathbf{v}_i = (d'_x(t), d'_y(t)), i = 1, 2, 3$.

## 4. General model for multiple-motions

We will first consider the case of only two motions. In this case, transparent, translucent, and occluded motions can be modeled by the equation

$$f(\mathbf{x}, t) = h(\mathbf{x} - t\mathbf{v}_2)g_1(\mathbf{x} - t\mathbf{v}_1) + g_2(\mathbf{x} - t\mathbf{v}_2) \quad (14)$$

where $\mathbf{x} = (x, y)$. This implies that $f(\mathbf{x}, t)$ is a solution of

$$\alpha(\mathbf{v}_1)\alpha(\mathbf{v}_2)\log|\alpha(\mathbf{v}_2)f|. \quad (15)$$

Eq. (15) can be derived in analogy to (8) and explains why traditional motion algorithms fail at occlusions - see below.

**Transparent motions** In case of transparent motions Eq. (14) reduces to

$$f(\mathbf{x}, t) = g_1(\mathbf{x} - t\mathbf{v}_1) + g_2(\mathbf{x} - t\mathbf{v}_2) \quad (16)$$

and Eq. (15) becomes

$$\alpha(\mathbf{v}_1)\alpha(\mathbf{v}_2)f = 0. \quad (17)$$

**Translucent motions** In this case Eq. (14) reduces to

$$f(\mathbf{x}, t) = g_1(\mathbf{x} - t\mathbf{v}_1)g_2(\mathbf{x} - t\mathbf{v}_2) \quad (18)$$

and Eq. (15) becomes

$$\alpha(\mathbf{v}_1)\alpha(\mathbf{v}_2)\log|f| = 0. \quad (19)$$

**Occluded motions** The occlusion of an image $\tilde{g}_1$, moving with velocity $\mathbf{v}_1$, by an image $\tilde{g}_2$, moving with velocity $\mathbf{v}_2$ and occlusion window $\chi$ (with values 0 or 1) is modeled as

$$\begin{aligned} f(\mathbf{x}, t) \quad &= (1 - \chi(\mathbf{x} - t\mathbf{v}_2))\tilde{g}_1(\mathbf{x} - t\mathbf{v}_1) + \\ &+ \chi(\mathbf{x} - t\mathbf{v}_2)\tilde{g}_2(\mathbf{x} - t\mathbf{v}_2) \end{aligned} \quad (20)$$

Eq. (20) is a particular case of Eq. (14) since $h(\mathbf{x}) = 1 - \chi(\mathbf{x})$, $g_1(\mathbf{x}) = \tilde{g}_1(\mathbf{x})$, and $g_2(\mathbf{x}) = \chi(\mathbf{x})\tilde{g}_2(\mathbf{x})$. The motion equation (15) simplifies to:

$$\alpha(\mathbf{v}_1)\alpha(\mathbf{v}_2)f = \pm\delta(B)\alpha(\mathbf{v}_2)f, \quad (21)$$

where $B$ is the occluding boundary. The above result can be derived by noting that since $\alpha(\mathbf{v}_2)f = h(\mathbf{x} - t\mathbf{v}_2))\alpha(\mathbf{v}_2)\tilde{g}_1(\mathbf{x} - t\mathbf{v}_1)$, we have

$$\begin{aligned} \alpha(\mathbf{v}_1)\alpha(\mathbf{v}_2)f &= \alpha(\mathbf{v}_1)h(\mathbf{x} - t\mathbf{v}_2)\alpha(\mathbf{v}_2)\tilde{g}_1(\mathbf{x} - t\mathbf{v}_1) \\ &= \delta(B)\alpha(\mathbf{v}_2)\tilde{g}_1(\mathbf{x} - t\mathbf{v}_1) \\ &= \delta(B)h(\mathbf{x} - t\mathbf{v}_2)\alpha(\mathbf{v}_2)\tilde{g}_1(\mathbf{x} - t\mathbf{v}_1) \\ &= \delta(B)\alpha(\mathbf{v}_2)f. \end{aligned}$$

Thus, motion estimation fails at occlusions because Eq. (17) is not valid at points on the occluding boundary and should be replaced by Eq. (21). Therefore, to estimate two motions at occlusions, we either (i) use Eq. (17) but do not integrate at occlusion points where we have motion discontinuities, or (ii) solve equation (21) to perform the estimation.

## 5. Solutions for $n$ transparent motions

Now suppose that $f$ is the additive superposition of $n$ motions with velocity $\mathbf{v}_i = (v_{ix}, v_{iy})$, i.e.,

$$f(x, t) = f_1(\mathbf{x} - \mathbf{v}_1 t) + \cdots + f_n(\mathbf{x} - \mathbf{v}_n t). \quad (22)$$

In this case, Eq. (17) becomes

$$\alpha(\mathbf{v}_1) \cdots \alpha(\mathbf{v}_n)f = 0. \quad (23)$$

We will now show how to estimate the multiple-motion parameters. First, we expand Eq. (23) to

$$\sum_I c_I f_I = 0 \quad (24)$$

where $I = (i_1, i_2, \ldots, i_n)$ are ordered sequences with elements $i_j \in (x, y, t)$ and $f_I$ are the partial derivatives of $f$ with respect to the elements in $I$. The mixed motion parameters $c_I$ are the coordinates of $\alpha(\mathbf{v}_1) \cdots \alpha(\mathbf{v}_n)$ in the canonical basis for differential operators (they are homogeneous symmetric functions of the coordinates of the motion vectors). With this notation, Eq. (24) can be rewritten as

$$\mathbf{LV} = \mathbf{0} \quad (25)$$

where $\mathbf{L} = (f_I)$ and $\mathbf{V} = (c_I)^T$. After multiplying Eq. (25) by $\mathbf{L}^T$ to obtain a $m \times m$ system of equations, we perform a weighted integration along a small neighborhood of the point in question, i.e. a convolution with a kernel $\omega(x)$,

$$\int \mathbf{L}(x)^T \mathbf{L}(x) \mathbf{V}(x) \omega(x)\, dx = \mathbf{0} \tag{26}$$

to make the system well posed. Since we are supposing that the motion vectors are locally constant, we can take $\mathbf{V}$ out of the integral and obtain

$$\mathbf{J}_n \mathbf{V} = 0 \tag{27}$$

where

$$\mathbf{J}_n = \int \mathbf{L}(x)^T \mathbf{L}(x) \omega(x)\, dx \tag{28}$$

We call $\mathbf{J}_n$ the *generalized structure tensor for $n$ motions.* Eq. (27) shows that the mixed motion parameters in $\mathbf{V}$ will form an eigenvector related to the zero eigenvalue of $\mathbf{J}_n$ and therefore can be computed in analogy to (11). More precisely, we have up to $m = \text{ord}(\mathbf{J}_n)$ different estimates for the mixed motion parameters given by

$$\mathbf{V}_i \propto (M_{im}, -M_{im-1}, \ldots, (-1)^m M_{i1}), \tag{29}$$

where $M_{ij}, i = 1, \ldots, m$ are the minors of $\mathbf{J}_n$ [12].

**Separation of the motion vectors** Now, we show how to recover the motion vectors $\mathbf{v}_1, \ldots, \mathbf{v}_n$ from their mixed coefficients $c_I$ in $\mathbf{V}$. Remember that $c_I$ are homogeneous symmetric functions of degree less than $n$ of the coordinates of the motion vectors . We interpret $\mathbf{v}_i$ as complex numbers, that is $\mathbf{v}_i = v_{ix} + j v_{iy}$, where $j^2 = -1$. In this case, the motion vectors will be the roots of a complex polynomial $Q_n(z)$ whose coefficients are functions of $c_I$:

$$Q_n(z) = z^n - A_{n-1} z^{n-1} + \cdots + (-1)^n A_0. \tag{30}$$

To compute the coefficients, we just note that $A_i$ are homogeneous symmetric functions of degree $n - i$ of $\mathbf{v}_1, ..., \mathbf{v}_n$. For example, the coefficients of $Q_n(z)$ for three motions are [12] $A_2 = c_{xtt} + j c_{ytt}$, $A_1 = c_{xxt} - c_{yyt} + j c_{xyt}$ and $A_0 = c_{xxx} - c_{xyy} + j(c_{xxy} - c_{yyy})$. For more motions, the coefficients of $Q_n(z)$ can be evaluated in analogy.

**Confidence measures** We have shown how to estimate multiple additive motions and now we consider the problem of detecting multiple motions, i.e., we want to quantify the confidence in the assumptions that we made.

In the case of one motion, the confidence is high if one eigenvalue of $\mathbf{J}$ is small and the other two are significant, i.e., rank$(\mathbf{J}) = 2$ [9]. This case excludes regions with aperture problems (two small eigenvalues) and occlusions etc. (three significant eigenvalues). With $n$ motions the confidence is still high if the rank$(\mathbf{J}_n) = m - 1$. Since with our new method we do not compute the eigenvalues, we need confidence measures that do not involve the eigenvalues.

The measures $K, S, H$ defined for $\mathbf{J}$ in (6) can be defined for $\mathbf{J}_n$ in analogy [12]. With these measures, the confidence criterion translates to $K = 0$ and $S \neq 0$. To compare $K$ with $S$, we found that $K^{1/m} \leq S^{1/m-1} \leq H$. This means that the confidence criterion ($K = 0$ and $S \neq 0$) becomes $K^{1/m} \ll S^{1/m-1}$ or, equivalently, $K^{1/m} < \epsilon S^{1/m-1}$.

**Algorithm 1** Hierarchical motion estimation

1: compute $\mathbf{J}_n$ according to Eq. (28)
2: **if** $K^{1/m} < \epsilon S^{1/m-1}$ (high confidence) **then**
3: compute $\mathbf{V}_1, \ldots, \mathbf{V}_m$ from the minors of $\mathbf{J}_n$ (Eq. (29))
4: compute the mixed motion parameters $\mathbf{V} = \alpha_1 \mathbf{V}_1 + \cdots + \alpha_m \mathbf{V}_m$
5: **if** n = 1 **then**
6: $\mathbf{v} = (V_x, V_y)$
7: **else**
8: $\mathbf{v}_1, \ldots, \mathbf{v}_n$ are the roots of $Q_n(z)$ in Eq. 30
9: **end if**
10: append treated pixel $x_0$ to list $L$
11: **end if**
12: **for all** $x_0 \notin L$ **do**
13: repeat steps 1 to 11 with $\omega(x - x_0) = 0,\ \forall x \notin L$
14: **end for**

**Low-complexity algorithms for multiple motions** Our hierarchical algorithm first evaluates the confidence in one motion and estimates that one motion in case of high confidence. Otherwise, the confidence for two motions is evaluated and two motions are estimated. This procedure can be iterated for up to $n$ motions. Moreover, motion at locations with low confidence is recomputed with a convolution kernel that integrates only locations with high confidence. This leads to correct solutions at occlusions, where confidence is low - see Fig. 1.

## 6 Results

In [12] we have presented results for up to three transparent motions of overlaid noise patterns. The results demonstrated high precision and a high spatial resolution of the estimated motion fields. Here we briefly illustrate the potential of our theoretical results for occluded motions - see Fig. 1.

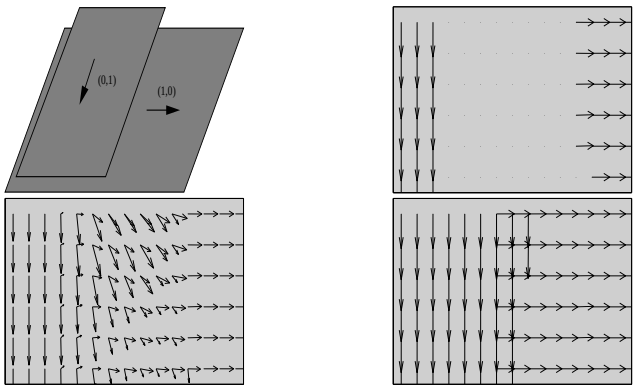


**Figure 1.** Simulation results obtained for two occluding layers of noise patterns with configuration shown top left. Result of using Eq. (17) with confidence measures according to Alg. 1 are shown top right: note that the occluding boundary has no confidence. Result of using the same Eq. (17) but ignoring the confidence measures are shown bottom left: in this case we solve for the wrong equation at the occluding boundary. The final result (bottom right) is obtained according to the first strategy described at the end of Sec. 4 with the boundary being defined as region of low confidence - see Alg. 1.

## 7. Summary and conclusions

We have argued that the intrinsic geometry of spatio-temporal patterns provides useful features that are unique in case of curvature. In addition, the curvature of image sequences can be used to estimate the parameters of motion.

Moreover, we have presented a general framework for estimation of single and multiple motions. The methods rely on derivatives, with an order that increases with the number of motions, but can be generalized to the use of more general linear filters [12]. In addition, we have shown how to detect multiple motions, i.e., we have derived confidence measures for the presence of multiple motions. We have obtained closed-form solutions for up to four transparent motions. For more than four motions, standard numerical methods for finding the roots of a polynomial can be used within our framework. Previous methods, however, relied on iterative solutions of high complexity that lacked a proof of convergence. For the case of single motions it had been shown before that the method for motion estimation based on the minors of the structure tensor **J** yields results that are better than those obtained by computing the eigenvalues and eigenvectors of **J** (and better than those based on the relations in Eq. 10). Traditional first- and second-order differential methods were also outperformed [3].

Finally, we have presented promising new results for the estimation of motions at occlusions and a hierarchical algorithm that can deal with both transparent and occluded motions.

## References

[1] D. Ballard and C. Brown. *Computer Vision*. Prentice Hall, Englewood Cliffs, New Jersey, 1982.

[2] J. L. Barron, D. J. Fleet, and S. S. Beauchemin. Performance of optical flow techniques. *IJCV*, 12(1):43–77, 1994.

[3] E. Barth. The minors of the structure tensor. In G. Sommer, editor, *Mustererkennung 2000*, pages 221–228. Springer, Berlin, 2000.

[4] E. Barth, T. Caelli, and C. Zetzsche. Image encoding, labelling and reconstruction from differential geometry. *CVGIP:GRAPHICAL MODELS AND IMAGE PROCESSING*, 55(6):428–446, 1993.

[5] E. Barth and M. Ferraro. On the geometric structure of spatio-temporal patterns. In G. Sommer and Y. Zeevi, editors, *Algebraic Frames for the Perception-Action Cycle*, pages 134–143, Berlin, 2000. Springer.

[6] E. Barth and A. B. Watson. A geometric framework for nonlinear visual coding. *Optics Express*, 7:155–185, 2000. http://www.opticsexpress.org/oearchive/source/23045.htm.

[7] M. J. Black and P. Anandan. The robust estimation of multiple motions: Parametric and piecewise-smooth flow fields. *Computer Vision and Image Understanding*, 63(1):75–104, 1996.

[8] G. H. Granlund and H. Knutsson. *Signal Processing for Computer Vision*. Kluwer, 1995.

[9] B. Jähne, H. Haußecker, and P. Geißler, editors. *Handbook of Computer Vision and Applications*, volume 2, chapter 13. Academic Press, Boston, 1999.

[10] S.-P. Liou and R. C. Jain. Motion detection in spatio-temporal space. *Computer Vision, Graphics, and Image Processing*, 45:227–50, 1989.

[11] C. Mota and E. Barth. On the uniqueness of curvature features. In G. Baratoff and H. Neumann, editors, *Dynamische Perzeption*, volume 9 of *Proceedings in Artificial Intelligence*, pages 175–178. Infix Verlag, 2000.

[12] C. Mota, I. Stuke, and E. Barth. Analytic solutions for multiple motions. In *Proceedings ICIP*, pages 917–920, 2001.

[13] B. Schutz. *Geometrical methods of mathematical physics*. Cambridge University Press, Cambridge, 1980.

[14] M. Shizawa and K. Mase. Simultaneous multiple optical flow estimation. In *Proc. IEEE Conf. Computer Vision and Pattern Recognition*, pages 274–8, Atlantic City, June 1990.

[15] E. P. Simoncelli. Distributed representation and analysis of visual motion. Technical Report 209, MIT Media Laboratory, Cambridge, MA, 1993.

[16] J. Y. A. Wang and E. H. Adelson. Representing moving images with layers. *The IEEE Transactions on Image Processing*, 3(5):625–638, 1994.

[17] W. Yu, K. Daniilidis, S. Beauchemin, and G. Sommer. Detection and characterization of multiple motion points. In *IEEE Conf. Computer Vision and Pattern Recognition*, volume I, pages 171–177, June 1999. Fort Collins, CO.

[18] C. Zetzsche and E. Barth. Direct detection of flow discontinuities by 3D curvature operators. *Pattern Recognition Letters*, 12:771–9, 1991.